JP Journal of Heat and Mass Transfer

https://pphmjopenaccess.com
https://doi.org/10.17654/0973576325046
Volume 38, Number 6, December 2025, Pages 863-895
P-ISSN: 0973-5763
E-ISSN: 3049-2556

DEVELOPMENT OF NEW ELEMENTS IN HEAT TRANSFER IN SOLIDS - THE THERMAL STRINGS MODEL

S. Veranoudis and S. Zoras

Department of Environmental Engineering
Democritus University of Thrace
Xanthi, Greece

Abstract

This study aims to calculate the final temperature distribution within a solid body and the time required for the body to reach a target (final) temperature. It examines both homogeneous and non-homogeneous solids, as well as hollow solid structures, including buildings. To analyse temperature distribution, duration of fluctuations, and energy transfer, a software application was developed specifically for this research. The results obtained from the application are compared with theoretical predictions. These theoretical calculations are based on classical heat diffusion theory as well as the thermal strings model, which is an extension of the Dual Phase Lag model. In the thermal strings model, the solid is treated as a pulsating thermal string, in which stationary thermal waves are generated.

Received: October 11, 2025; Accepted: November 21, 2025
Keywords and phrases: dual phase lag, heat transfer, thermal strings, non-Fourier heat conduction, system of temperature variations.

How to cite this article: S. Veranoudis and S. Zoras, Development of new elements in heat transfer in solids - the thermal strings model, JP Journal of Heat and Mass Transfer 38(6) (2025), 863-895. https://doi.org/10.17654/0973576325046

Published Online: December 11, 2025

1. Introduction

Three main models describe heat transfer in solids: the Fourier heat diffusion model, the Cattaneo-Vernotte thermal wave model, and the dual phase lag (DPL) model. The Fourier model (diffusion) computes the final temperature of the body, which in homogeneous solids is represented by the average temperature of all sides.

In contrast, the Cattaneo-Vernotte and DPL models characterize heat transfer as a process involving thermal waves [1, 2] that work to eliminate temperature differences and drive the solid toward thermal equilibrium [3]. The solid has thermal inertia [4], which accounts for the characteristic delay times $(\tau_o$ and $\tau_T)$ between the onset of heat and the corresponding temperature change [5]. The DPL model expands upon the Cattaneo-Vernotte framework.

The equations of the three models are as follows:

$$q = -k_\sigma \cdot \nabla u, \text{ (Fourier)}, \tag{1}$$

$$q + \tau \cdot \frac{\partial q}{\partial t} = -k_\sigma \cdot \nabla u, \text{ (Cattaneo-Vernotte)}, \tag{2}$$

$$q + \tau_o \frac{\partial q}{\partial t} = -k_\sigma \left(\nabla u + \tau_T \frac{\partial}{\partial t} (\nabla u) \right), \text{ (DPL)}. \tag{3}$$

The DPL equation (3) along with the conservation of energy equation $\nabla q = -\rho c_{sp} \frac{\partial u}{\partial t}$ leads to the following result:

$$\frac{\partial^2 u}{\partial t^2} + \frac{1}{\tau_o} \frac{\partial u}{\partial t} = c^2 \nabla^2 u + c^2 \tau_T \frac{\partial}{\partial t} (\nabla^2 u). \tag{4}$$

Here $c = \sqrt{\frac{k_\sigma}{\rho c_{sp} \tau_o}}$ represents the velocity of heat propagation through the material.

In this context, ρ denotes the material's density (kg/m^3). c_{sp} signifies the specific heat capacity $(\mathrm{J} \cdot \mathrm{K}^{-1} \cdot \mathrm{kg}^{-1})$.

There exists a conflict between the diffusion and wave models in heat transfer theory. The DPL model accurately calculates the time required for thermal equilibrium but falls short in explaining the phenomenon where certain areas maintain a fixed temperature and remain in a steady state, even as heat propagates through them via wave mechanisms (including particle oscillations and collisions). In homogeneous solids, these regions are typically located in the middle area of the material.

2. Diffusion Model and Thermal Strings Model

2.1. Time, energy and temperature oscillations

Two phenomena must be reconciled: the finite velocity of thermal signals (as described by the DPL model) and the existence of points with fixed and steady temperatures (as represented by the diffusion model).

Another potential issue is that, according to the DPL model, heat wave propagation occurs over very short time periods, after which the material's behavior shifts towards favoring heat diffusion. How can this change in the material's behavior be explained?

An effective approach to resolving this issue is to consider that the two lag times are equal $(\tau_o = \tau_T)$. The equations

$$q(r, t_q) = -k_\sigma \nabla u(r, t_T),$$

$$q(r, t + \tau_o) = -k_\sigma \nabla u(r, t + \tau_T)$$

become identical, which implies that the time needed for equilibrium is also the same. When $\tau_o = \tau_T$, wave regression occurs due to inertia, resulting in a reverse heat wave that propagates backwards. The initial wave interacts with this reverse wave, producing stationary thermal waves. The axis along which this interaction takes place can be conceptualized as a pulsating thermal string, where stationary thermal waves are formed. The temperature fluctuations are derived from the interference of heat waves in three dimensions. It has been mathematically demonstrated that the "oscillations"

in temperature of each particle are critically damped until they reach their final value.

By solving equation (4), it is obtained an analytical solution that describes the "distance" f of a point from its final temperature. This solution applies separately for each axis and incorporates both the time and position of each point, depending on the boundary and initial conditions. The one-dimensional solution is given by the equation:

$$f_x(t,\, x) = u(t,\, x) - u_{fx} = \Theta_{ox}\left(1 + \frac{m^* \cdot t}{\tau_o}\right) e^{-\frac{m^* \cdot t}{\tau_o}} \cdot \cos(b_x x + \varphi_o). \qquad (5)$$

The coefficients in the previous equation take the following values:

(1) If the opposite faces are free to balance, then

$$\Theta_{ox} = u_{hx} - u_{fx}, \quad \lim_{t\to\infty} u(t,\, x) = u_{fx} = \frac{u_{hx} + u_{cx}}{2},$$

$$m^* = 1, \quad b_x = \frac{\pi}{w \cdot L_x}, \quad w = 1, \quad \varphi_o = 0.$$

(2) If the opposite faces have constant temperatures (no "t" time exists), then

$$\Theta_{ox} = u_{hx} - u_{fx}, \quad \lim_{t\to\infty} u(t,\, 0) = u(0,\, 0), \quad \lim_{t\to\infty} u(t,\, L_x) = u(0,\, L_x),$$

$$m^* = 0, \quad b_x = \frac{\pi}{w \cdot L_x}, \quad w = 1, \quad \varphi_o = 0.$$

(3) Only the face $x = 0$ has steady temperature:

$$\Theta_{ox} = u_{cx} - u_{fx} = u_{cx} - u_{hx}, \quad \lim_{t\to\infty} u(t,\, x) = u_{fx} = u_{hx},$$

$$m^* = 1, \quad b_x = \frac{\pi}{w \cdot L_x}, \quad w = 2, \quad \varphi_o = \frac{3\pi}{2}.$$

(4) Only the face $x = L$ has steady temperature:

$$\Theta_{ox} = u_{hx} - u_{fx} = u_{hx} - u_{cx}, \quad \lim_{t\to\infty} u(t,\, x) = u_{fx} = u_{cx},$$

$$m^* = 1, \quad b_x = \frac{\pi}{w \cdot L_x}, \quad w = 2, \quad \varphi_o = 0.$$

Similar equations describe thermal standing waves in the other axes as well. The symbols that appear in the equations are:

Nomenclature

t = time (sec)

τ_o = characteristic response time of the material (sec)

u = temperature (K)

u_{fx}, u_{fy}, u_{fz} = final temperature in each direction (K)

f_x, f_y, f_z = the difference of a point's temperature from its final temperature (K)

$\Theta_{ox}, \Theta_{oy}, \Theta_{oz}$ = maximum temperature difference from the final temperature (K)

$u_{hx}, u_{hy}, u_{hz}, u_{cx}, u_{cy}, u_{cz}$ = temperatures of hot and cold faces in 3 axes (K)

L_x, L_y, L_z = the thickness of the material in every direction (m)

A_{xy}, A_{xz}, A_{yz} = cross-sectional areas (m^2)

ρ = density $(\mathrm{kg/m}^3)$

k_σ = the coefficient of thermal conductivity (W/m/K)

c_{sp} = the specific heat $(\mathrm{J \cdot K^{-1} \cdot kg^{-1}})$

Q_x, Q_y, Q_z = heat transferred in 3 axes (J)

The total temperature difference of each point from the final value will be the average of the three differences. So for each point the following will apply

$$f(t, x, y, z) = \frac{f_x(t, x) + f_y(t, y) + f_z(t, z)}{3}, \tag{6}$$

with

$$t \geq 0, \quad 0 \leq x \leq L_x, \quad 0 \leq y \leq L_y, \quad 0 \leq z \leq L_z.$$

The characteristic time (for each thermal string) is

$$\tau_o = \frac{\rho c_{sp}}{k_\sigma b^2} \tag{7}$$

$\left(b = \frac{\pi}{wL},\ b \text{ is different for each axis} \right)$.

By applying the analytical solution to equation (3), the heat flux across a cross-section of the body can be determined. Depending on the boundary conditions, it is subsequently feasible to calculate the energy and power transferred from one end of the body to the other.

In the case of Dirichlet boundary conditions, the boundaries will maintain a steady temperature. Conversely, under Neumann boundary conditions, there will be a constant heat flux. For a perfectly insulated body, the heat flux will be zero.

So,

$$q(0) = q(L) = \frac{\partial u(0)}{\partial x} = \frac{\partial u(L)}{\partial x} = 0.$$

The diffusion model and the thermal strings model yield the same results while describing distinct heat transfer mechanisms. The thermal string equation that meets the specified boundary conditions corresponds to Case (1) of equation (5). In classical diffusion theory, the solution that complies with these boundary conditions is represented by the known distribution, utilizing the error function $f = \Theta_o \left[1 - erf\left(\frac{x - \frac{L}{2}}{2\sqrt{at}} \right) \right]$. This equation illustrates the temperature distribution when two bodies (one hot and one cold) are in contact at $x = L/2$. Initially, the distribution exhibits a sigmoid shape, transitions to linear, and ultimately becomes a flat line.

Conversely, the distribution in the thermal strings model takes on a sinusoidal shape before also settling into a flat line.

The time required for the solid to reach thermal equilibrium is consistent across both models. Given these boundary conditions, this time is represented as $t_f = \frac{L^2 \rho c_{sp}}{k_\sigma} = \pi^2 \tau_o = 9.86\tau_o$. The differing shapes of the temperature distribution in the diffusion and thermal strings models suggest a variation in the amount of stored energy between the two approaches. Specifically, the thermal strings model indicates approximately 27% more thermal energy on the hot side and 27% less on the cold side compared to the classical model. This discrepancy is significant only when the two parts are allowed to equilibrate, as it influences the calculation of the transferred energy within the body, without affecting the external heat load required for heating or cooling.

A solid body may consist of multiple layers of materials along the *x*-axis. If these layers are in a steady state with fixed temperatures, constant heat transfer is necessary to maintain these temperatures at both ends. The heat transferred and the power required along this axis are detailed in the table below (R here is the thermal resistance of each material with units (m^2K/W) and it is the reciprocal of the material's U_{VALUE}):

Table 1. Power required for non-equilibrium

$\overline{\dot{Q}_x} = kA_{yz}\frac{2\Theta_{ox}}{3L_x} = \frac{1}{\sum R_x}L_yL_z\frac{2\Theta_{ox}}{3}$
$\overline{\dot{Q}_y} = kA_{xz}\frac{2\Theta_{oy}}{3L_y} = \frac{1}{\sum R_y}L_xL_z\frac{2\Theta_{oy}}{3}$
$\overline{\dot{Q}_z} = kA_{xy}\frac{2\Theta_{oz}}{3L_z} = \frac{1}{\sum R_z}L_xL_y\frac{2\Theta_{oz}}{3}$

The $\sum R_x$ resistance is calculated by considering the resistances of the layers as connected in series, while $\sum R_y$ and $\sum R_z$ are treated as connected in parallel, much like an electric circuit $\left(\frac{1}{\sum R_y} = \frac{1}{R_1} + \frac{1}{R_2} + \cdots\right)$.

It is important to note that the thermal string model yields results comparable to the classical model for most calculated values.

Specifically, the duration of heat transfer between two solids in contact is nearly identical, differing by only 0.056% from the classical theory.

Similarly, the heat loads necessary to maintain non-equilibrium conditions are also consistent, differing by just 0.051%.

Furthermore, the final temperature distribution across the solid remains the same in both models.

2.2. The molecular vibrations

When heat transfers from one point to another, a portion of it becomes absorbed at the new location, resulting in an increase in temperature, while the remaining heat continues to propagate to the next point. The product ρc_{sp}, describes the capacity to store energy at a specific point and plays a crucial role in determining the characteristic time, τ_o, while k_σ represents the capacity to transfer heat to the subsequent point. These two phenomena operate in a competitive manner. If ρc_{sp} equals zero, then τ_o is also zero, indicating that no time is required to reach the final temperature. Conversely, if k_σ equals zero, there would be no conductivity, leading to an infinite recovery time.

The process of energy transfer and storage is intricate. Each molecule gains kinetic energy, resulting in heightened thermal motion. On a macroscopic level, this translates to an increase in temperature. Concurrently, the frequency of collisions between neighboring molecules rises, which contributes to the transfer of heat and can be understood as “conductivity.” Once the molecules in a given region reach their final temperature, additional heat does not accumulate; instead, it is transferred to neighboring regions through collisions. In a theoretical sense, the entire system can be likened to Newton’s Cradle on a local scale (Figure 1).

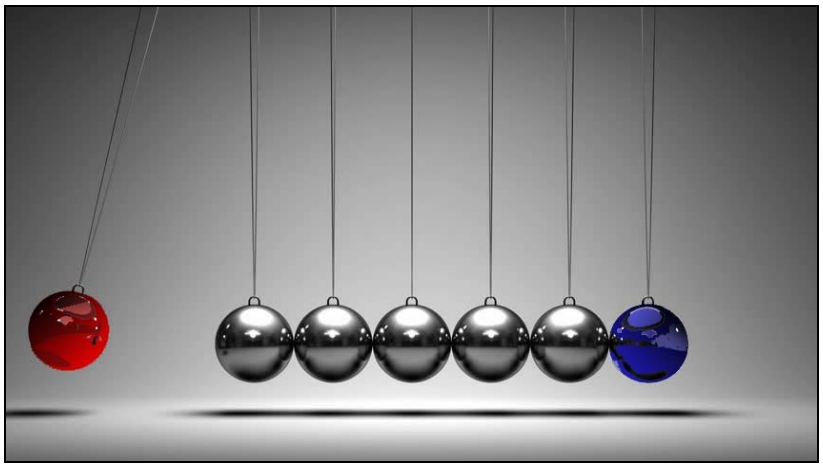

Figure 1. Newton's cradle and energy transfer.

Why do the molecules in a region that has reached thermal equilibrium stop absorbing heat? The product ρc_{sp} does not vanish, even though it has been observed that the specific heat capacity varies with temperature. The key reason is that no further heat transfer occurs in the region due to the absence of temperature differences with neighboring molecules. This phenomenon is limited to the initial set of molecules and not the subsequent ones. If it occurred with the following molecules, then there would be no need for heat to propagate forward. How do molecules with "medium" temperature determine which neighboring molecules to interact with? In situations of forced heating, the molecules continuously absorb some heat while simultaneously transferring more of it to their neighbors.

The regulator and controller of heat absorption and conduction is the function $f(x, y, z, t)$, which represents the distance from the final temperature. When one side of a solid is maintained at a constant temperature, the entire body will eventually reach that temperature, occurring simultaneously throughout all areas via steadily decreasing oscillations. The only scenario in which a solid with varying temperatures on opposite sides has points that remain unaffected by heat transfer is when all sides are allowed to equilibrate freely. In this instance, some points already have

attained their equilibrium temperature and will show no changes. These are points characterized by minimal entropy and a perfectly oriented heat flow.

3. System of Temperature Variations [SoTV]

The system of temperature variation (SoTV) is a software application developed in Python that utilizes the principles of thermal strings theory to calculate various parameters of solid bodies, including temperature, energy, power, thermal resistance, U_{VALUE}, and relaxation time, which is essential for determining the time needed to reach an equilibrium state. Additionally, the application predicts whether the final state of the body will be in equilibrium or non-equilibrium. Designed to display colorful 3D heat maps, SoTV also offers users the ability to regulate and input temperature within a building as well as its surrounding environment.

The solid body is divided into numerous small pieces, referred to as elements. Based on the desired precision, the solid can be subdivided into (i) $16^3 = 4096$ (ii) $21^3 = 9261$ or (iii) $26^3 = 17576$ elements. For each element, there is data on its center position, its size, and its initial temperature. Using the analytical equations derived from thermal strings theory, the final temperature of each element was computed. The thermal behavior of each element is organized within matrices.

There exists an array containing sub-arrays with five dimensions. The first three dimensions represent the position (x, y, z) of each element, the fourth dimension corresponds to its temperature, and the fifth dimension denotes time (t).

Then, input the temperatures (Figure 2) on the surfaces of a parallelepiped, specify its dimensions and layers, define the thermal conductivity coefficient for each layer, and indicate whether the software should account for the thermal resistance due to convection at the solid's surface in contact with the air (transition resistance).

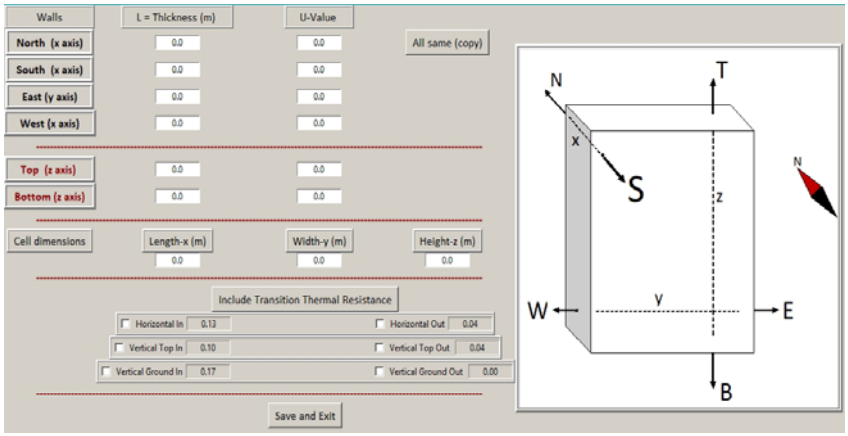

Figure 2. SoTV (body properties window).

A significant challenge in software that models dynamic systems is the temporal variation of their parameters [6, 7]. The most common approach to determine the time required for a system to reach a final steady state [8] is the time step method. In all such methods, a fixed time step is established, and the functions are recalculated iteratively [9].

The SoTV software employs the "Half Step Method," which operates as follows:

Initially, determine the temperature on all six sides of a solid, which may or may not be homogenous. Utilizing the theory of thermal strings, it is feasible to compute the final temperature at all points within the solid. This calculation involves finding the limit of temperatures after an infinite duration, expressed as $\lim_{t\to\infty} u(t, x, y, z)$.

Starting from the final temperature that the elements achieve after an exceedingly long time, work the way backwards. Time steps are implemented, where each step is half the duration of the previous one. Then, continue taking successive steps backward as long as the temperature values in the arrays remain equal to the final values. If they remain equal, then should proceed further back; however, if they diverge, then make half steps forward.

Through a series of small, repeated steps both forward and backward in time, the exact moment is pinpointed when thermal fluctuations cease. By analyzing the time equations and using the last values of the fluctuations, the elapsed time is calculated, this time based on the initial conditions. Thus, it was determined how long it takes for a given initial temperature distribution to reach a final state.

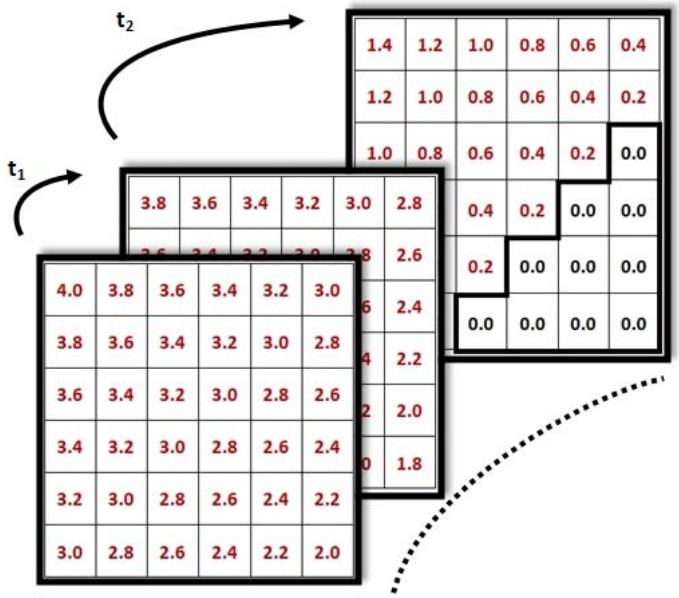

Figure 3. Time depended data of elements' temperature.

In Figure 3, it can be observed a representation of temperature values for various elements of the body. Over time, the "distance" of the temperature from the final value decreases, ultimately reaching zero. This indicates the moment when the area has attained the "target temperature," after which it will stabilize in a steady state.

In Figure 4, the blue steps represent the forward movement in time, while the red ones signify the backward movement. Each step represents a certain duration and is half the length of the preceding one. The white dot indicates the moment when the solid reaches equilibrium. After this point (occurring at the sixth step), the temperature in any area remains stable.

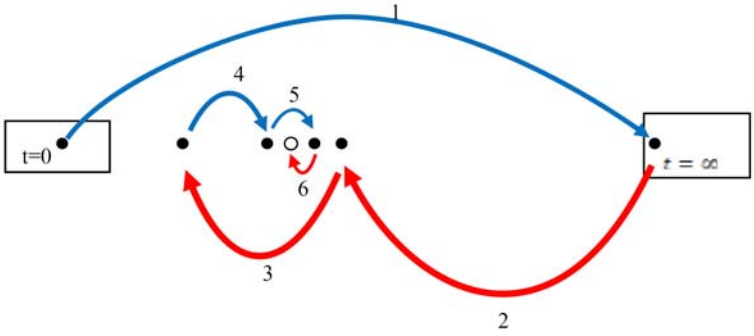

Figure 4. "Half step method".

SoTV conducts multiple calculations where each iteration halves the time. As a result, the time steps progressively become smaller. A significantly large initial time value is set (10^8 times greater than the characteristic time, τ_o). There is also flexibility to set the precision of our calculations, allowing the time subdivisions to become extremely small (high precision) or relatively larger. This leads to accurate timing with designated "time step minimum" (tsm): $tsm = \frac{10^8}{2^{29}}\tau_o \cong 0.19\tau_o$ or $tsm = \frac{10^8}{2^{33}}\tau_o \cong 0.012\tau_o$ or $tsm = \frac{10^8}{2^{36}}\tau_o \cong 0.0015\tau_o$.

In addition to the precision of the minimum time step, which dictates how closely to approximate the correct time, the accuracy of temperature measurements is also crucial. Measurements may have a tolerance that constitutes a fraction of the final temperature range. For instance, when considering buildings at ambient temperatures, the calculation error can be around $\pm 10^{-20}$C.

It is important to remember that the final temperature values at all points in the solid, according to the theory of thermal strings, resulting from a diminishing oscillation of thermal variations. In theory, these oscillations can persist indefinitely. This implies that if aiming to ascertain temperature

values with extreme precision, then the relaxation time may become infinite. Consequently, a computing system that tracks micro-variations will never truly recognize that a solid has reached equilibrium [10].

To enhance the speed of certain calculations, specific points of interest was selected. By focusing on 27 distinct points rather than evaluating all the thousands of elements within the solid, could significantly reduce computation time. These points include (i) the vertices of the parallelepiped, (ii) the midpoints of its edges, and (iii) the centers of its surfaces (Figure 5).

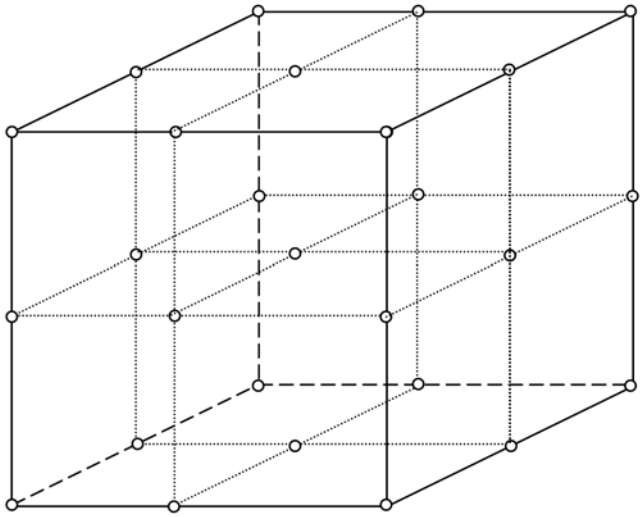

Figure 5. SoTV (key points of a solid).

The interplay of fluctuations across the three axes creates a superimposition of heat waves. This phenomenon implies that there are no "hidden" points in between that would continue to exhibit wavelike thermal fluctuations while the 27 control points have already ceased to do so. Consequently, our calculations can be deemed accurate.

Boundary conditions play a crucial role in the heat transfer process, necessitating that the user specifies whether the temperature remains steady or varies on each face of the body [11, 12]. This steadiness is represented as a Boolean parameter, which influences both time and energy calculations.

In cases where the body comprises multiple layers, the temperature gradient will vary along the axis at the boundaries of each layer (see Figure 6).

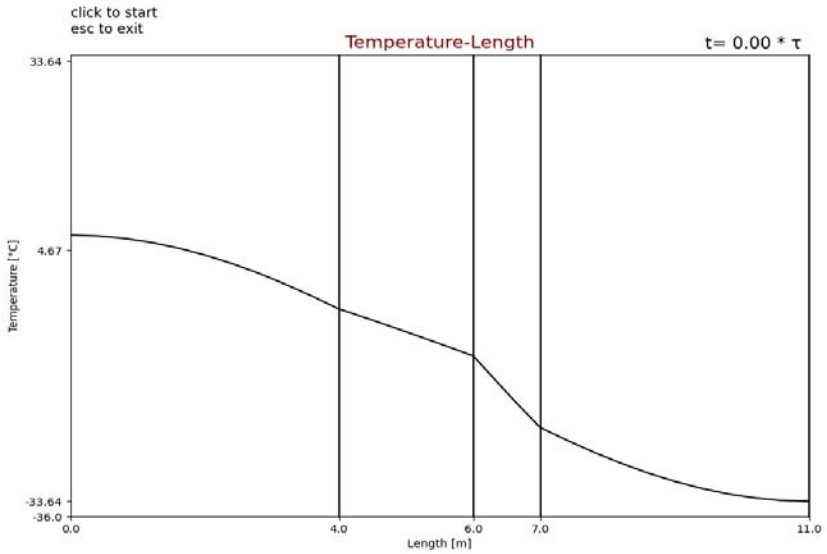

Figure 6. Temperature distribution in a 4-layers solid body.

In cases where the body comprises multiple layers, the temperature gradient will vary along the axis at the boundaries of each layer (see Figure 7).

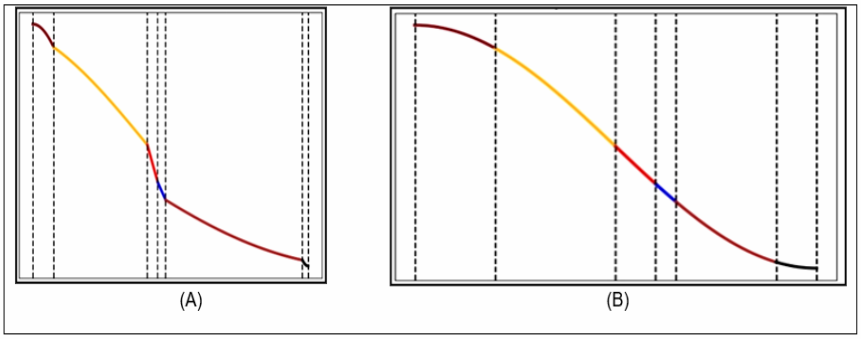

Figure 7. (A) Real and (B) Equivalent dimensions and temperature distribution in a multilayer body.

Someone could use an equivalent length (or thickness) of the body so that the temperature distribution inside it has sinusoidal shape.

4. Results (Calculations and Measurements)

4.1. Time

The relaxation time predicted by the thermal string model for a free-to-equilibrate solid is given as $t_f = \pi^2 \tau_o = 9.86\tau_o$. When one side of the solid is maintained in a steady state, the body will reach its final condition after $t_f = 4\pi^2 \tau_o = 39.47\tau_o$ which is four times greater than the previous value. Here, $\tau_o = \frac{\rho c_{sp}}{k_\sigma b^2}$ represents the characteristic time, where ρ is the density of the material, c_{sp} is the specific heat capacity, k_σ is the coefficient of thermal conductivity, and $b = \frac{\pi}{L}$.

The results obtained have been compared from the application with those predicted by the thermal string model. The time metrics involve assessing the following factors: calculation accuracy, the temperature difference between opposite sides, the status of the sides in steady state, and their deviation from the predicted theoretical values.

(1) The accuracy level of calculations performed by our computer does not significantly impact the results. For instance, if the relaxation time is approximately one minute, the deviation (or error) is about 0.1 seconds. For longer relaxation times, the discrepancy increases but remains relatively insignificant; for a relaxation time of one day, the calculation error amounts to about 15 minutes.

(2) There is a notable divergence between theoretical results and practical applications when the initial temperatures are in close proximity to their final values, compared to situations where the temperatures are significantly distant from u_f.

For temperatures that are very near the final value, the equilibrium recovery time is less than the threshold of $t_f = \pi^2\tau_o = 9.86\tau_o$, beginning at $t = 4.09\tau_o$ and increasing rapidly. As the temperature difference across the opposing sides increases, the recovery time stabilizes around $t = 10.00\tau_o$ (as illustrated in Figure 8), even when the temperature differences Δu reach thousands of degrees.

In cases of huge temperature differences occurring along a single axis (while the other axes remain at a uniform temperature) the solid behaves similarly to a steady-state condition rather than a free one. Consequently, the recovery time tends to extend to $t = 40.00\tau_o$ or even surpass that value.

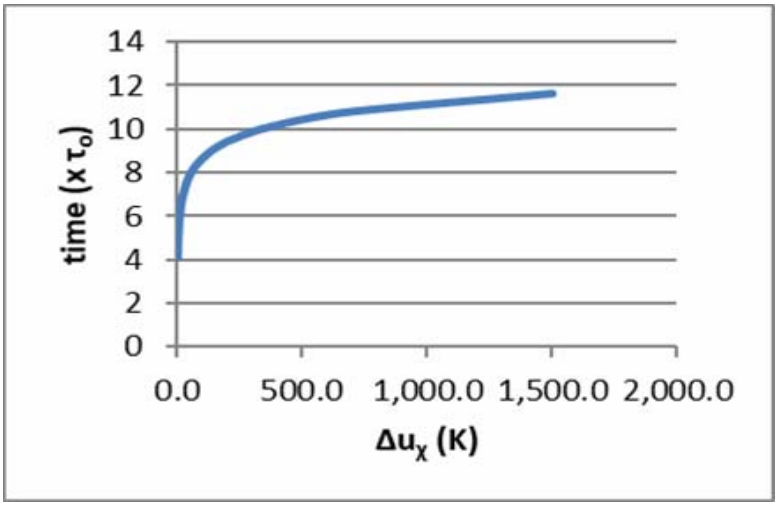

Figure 8. Relaxation time $(\Delta u_x \leq 1500^{\circ}\mathrm{C})$ - SoTV.

(3) For random temperature values observed at six sites within a solid, where none of the sites has a stabilized temperature, the outcomes align with the predictions of thermal strings theory. Specifically, most recovery times for the final temperature are approximately $t_f = \pi^2\tau_o = 9.86\tau_o$. This pattern emerges consistently across a substantial number of measurements (Figure 9(a)).

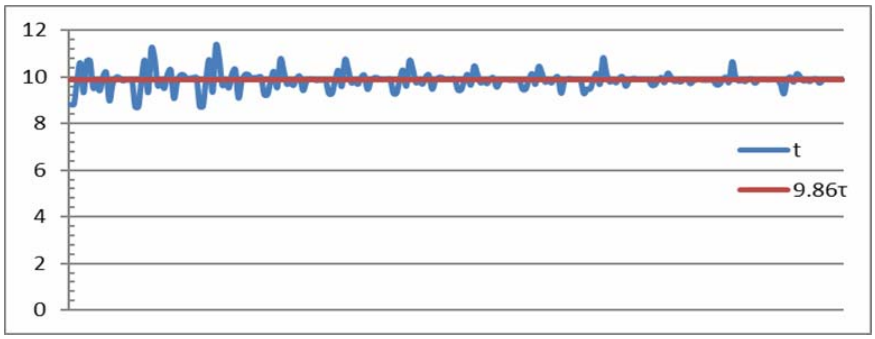

(a)

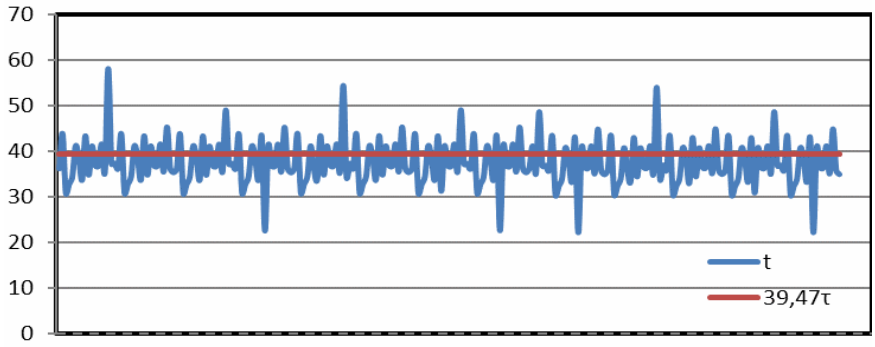

(b)

Figure 9. Relaxation time with random face temperatures – SoTV.

When the temperature is maintained at a fixed value on one side, the solid takes longer to reach its final state, with a recovery time of approximately $40\tau_o$. This aligns with the value predicted by thermal strings model $(t_f = 4\pi^2\tau_o \approx 39.47\tau_o)$ as shown in Figure 9(b).

(4) Additionally, when the initial temperatures are significantly distant from the final value, the recovery time appears to increase, as the solid has a longer journey to reach equilibrium. The results depicted in Figure 9(a) and Figure 9(b) are in close agreement with the predicted values. If the initial temperature is near the final state, the time required for recovery decreases; conversely, if it is far from the final temperature, the recovery time increases.

4.2. The final condition

The final state of the body can either be in equilibrium or non-equilibrium, and this determination is entirely dependent on the boundary conditions. Each surface of the solid may have a fixed temperature or be allowed to reach any temperature it desires. For the body to be constrained, it requires energy that must be either supplied to or extracted from it. In other words, an external mechanism is necessary to maintain a constant temperature on one side, typically utilizing a thermostat.

In the accompanying color maps, the white areas represent the geometric locus of points that exhibit the average temperature across the six surfaces of the body. Hot spots are depicted in red and cold spots in blue. The figures on the left illustrate the initial state of the body, while those on the right demonstrate the final state as influenced by the boundary conditions. In Figure 10(a), where all sides are free, the final temperature of every part of the body aligns with the average temperature, resulting in the entire area appearing white.

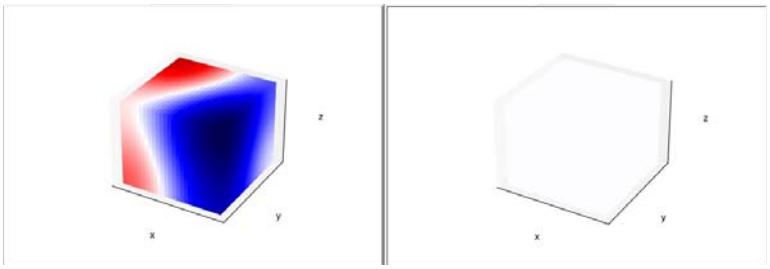

Figure 10(a). Initial and final conditions with 6 free sides.

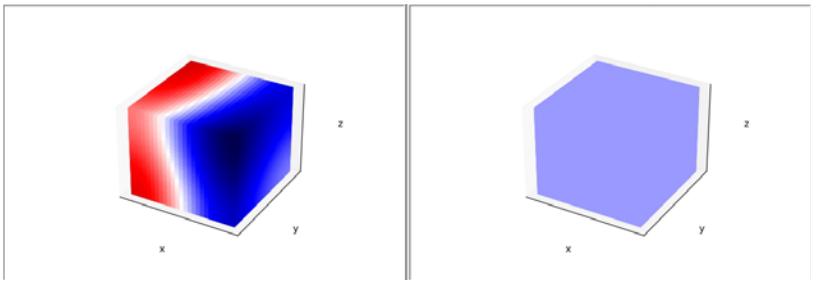

Figure 10(b). Initial and final conditions with 5 free and one (cold) fixed side.

If stability is maintained on just one of the six sides, then the body achieves equilibrium once more. When the constant temperature side is cold, the entire body reaches a uniform cold equilibrium (see Figure 10(b)). Eventually, the flow of energy between different areas within the body ceases.

Finally, this case expends energy to maintain a constant temperature, keeping it unchanged in relation to the environment. However, this does not pertain to the inner part of the body or the energy flow to other areas.

In the figures below, it is illustrated the same initially solid body in its final states with varying fixed sides: two sides (Figure 10(c)), three sides (Figure 10(d)), four sides (Figure 10(e)), five sides (Figure 10(f)), and six sides (Figure 10(g)).

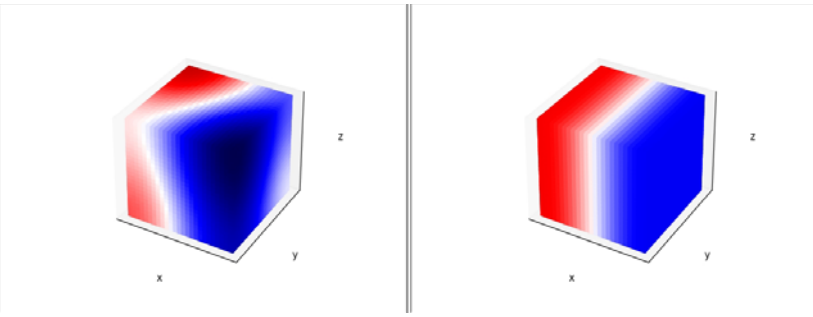

Figure 10(c). Initial and final conditions with 2 (opposite) fixed sides.

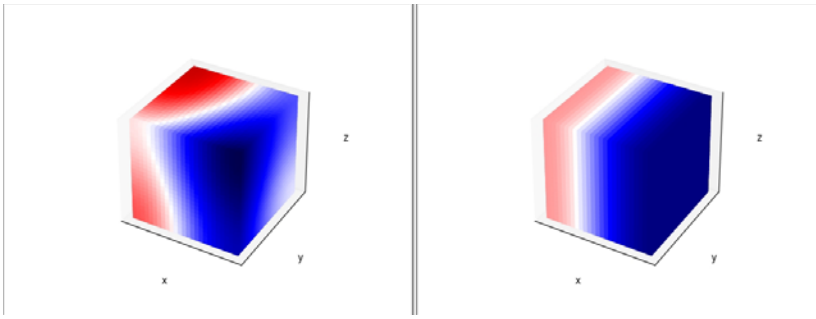

Figure 10(d). Initial and final conditions with 3 (2 opposite) fixed sides.

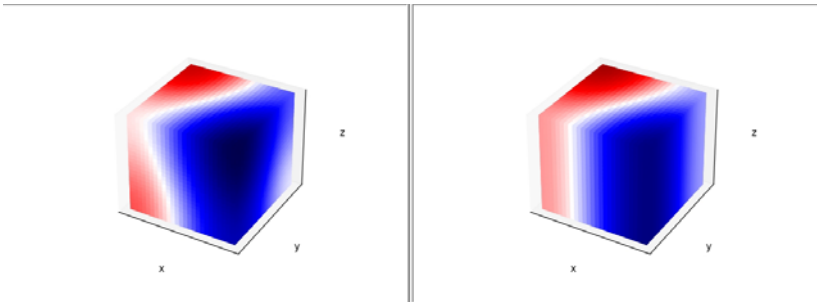

Figure 10(e). Initial and final conditions with 4 fixed sides.

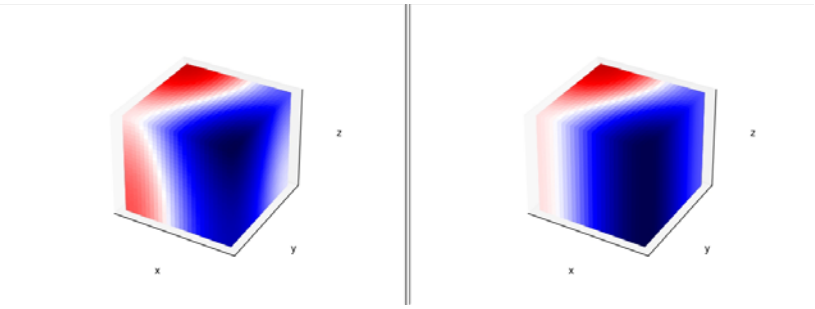

Figure 10(f). Initial and final conditions with 5 fixed sides.

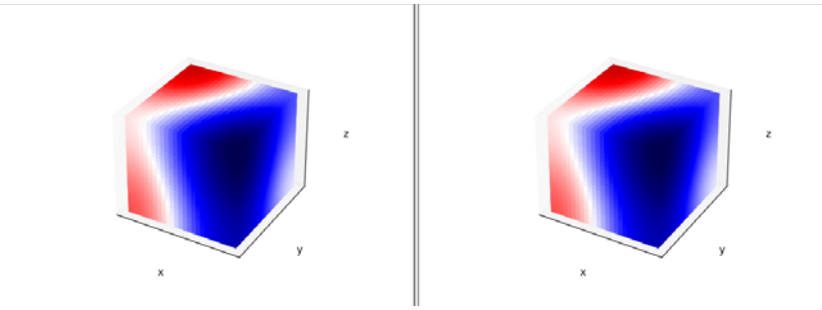

Figure 10(g). Initial and final conditions with 6 fixed sides.

4.3. Energy and power

The energy transferred depends on time, while the power required is not. The energy relies entirely on the dimensions of the body, as it is stored within its structure. According to SoTV, in large bodies that are allowed to equilibrate, the energy transferred between hot and cold regions is

proportional to both the dimensions and the material's storage capacity. This indicates that the transferred energy is influenced by the heat capacity [13].

Furthermore, the total energy transferred does not rely on the coefficient of thermal conductivity; this coefficient affects only the velocity of transfer, not the overall heat load.

As anticipated, there is a clear dependence of the transferred energy on the temperature difference between the sides. Smaller temperature differences result in a lesser amount of energy being conveyed along an axis. In fact, only $1/3$ of the temperature difference between opposite sides contributes to the energy transfer, since other sides also influence the temperature in a given area. Consequently, thermal pulses originating from one side of a body are transmitted with reduced amplitude to the other side, making them less perceptible.

If one side of a body is maintained at a constant temperature, then it requires four times more energy to achieve thermal balance with the opposite side compared to a scenario where it is free to vary.

The power needed to sustain one side at a fixed temperature while allowing the other side to fluctuate depends on several key factors:

(i) From the cross-sectional area. The size of the dividing surface between the two areas significantly impacts power consumption. A larger area necessitates more energy transfer.

(ii) From thermal resistance. High thermal resistance facilitates maintaining a temperature difference across the body. Increased resistance hinders the efficient transfer of heat.

(iii) The characteristic time is crucial in determining the required power. A change in length can markedly affect all relevant quantities. Shorter distances between the walls of a body require greater power, as thinner walls are more conductive. For example, doubling the thickness of the walls results in a transfer time that is four times longer.

The type of materials (and their properties) used can influence the amount of energy required [14, 15]. While the heat capacity of a material is significant in creating a temperature difference between the two sides, it becomes less relevant once that difference is established. To maintain the difference, only the coefficient of thermal conductivity remains important.

5. Building's Application

5.1. The building as a circuit

The envelope of a building comprises walls constructed from multiple layers of materials. The complexity of this layering in masonry makes it challenging to calculate the energy transfer through the structure.

Consider a vertical wall within the building, where the indoor temperature differs from that outside. Each layer possesses its own thermal resistance and facilitates heat transfer in distinct ways. In addition to the arrangement of these resistances, the vertical and horizontal composition of materials also plays a role. For instance, the temperature at the top of the wall may vary from that at the bottom, which is in contact with the ground.

When heat flows through a wall along the x-axis, it encounters thermal resistances that are arranged in series, while along the other axes, these resistances are configured in parallel. This distinction affects the total resistance in each direction. The primary challenge in heat flow arises from the series resistances, rather than the parallel ones. As a result, the time required to achieve thermal equilibrium is predominantly determined by the x-axis, since equilibrium is reached more rapidly along the other axes.

Each wall can be likened to an electrical circuit (Figure 11). In this analogy, heat (similar to electric current) flows more readily through parallel resistors. Additionally, the temperature difference across the wall is analogous to an electric potential difference (voltage).

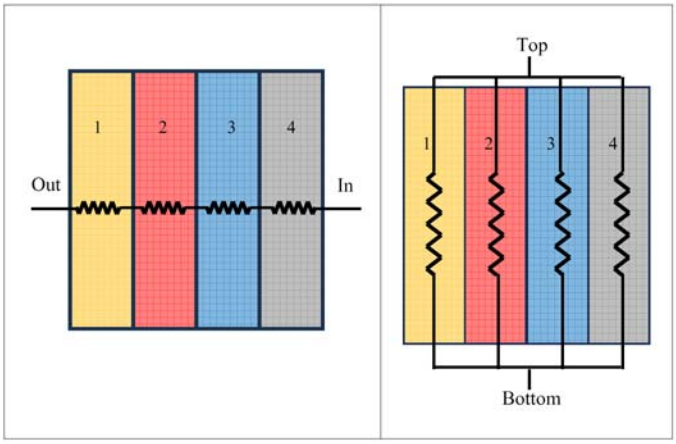

Figure 11. Thermal resistance of a wall.

Each wall not only represents electrical resistance but also contains a capacitor, which indicates its ability to store energy, and a coil, which reflects the thermal inertia of the materials in response to temperature changes (Figure 12).

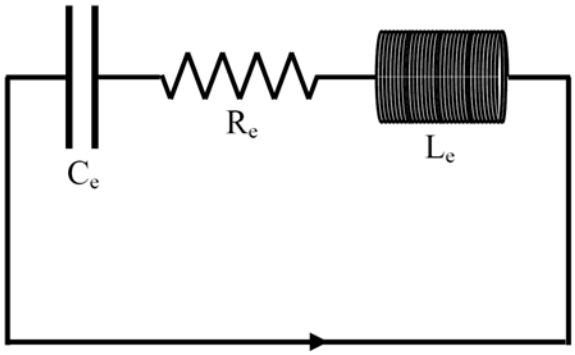

Figure 12. RLC circuit.

The equation which describes the circuit is

$$V_L + V_R + V_C = 0 \Rightarrow L_e \frac{dI(t)}{dt} + I(t)R_e + \frac{1}{C_e}\int_0^t I(t)dt$$

$$\Rightarrow \ddot{I}(t) + \frac{R_e}{L_e}\dot{I}(t) + \frac{1}{L_e C_e} I(t) = 0. \tag{8}$$

The solution to this equation describes a damp electrical oscillation, which can be categorized as over-damped, under-damped, or critically damped. In critically damped oscillations, the system reaches its final state via the shortest possible path. Conversely, in over-damped oscillations, the system will never achieve the final condition, while under-damped oscillations will reach the predetermined state, albeit after a considerable amount of time.

In a circuit with a variable frequency source, the circuit's behavior is influenced by the capacitive and inductive reactance. When the capacitive impedance (X_C) is greater than the inductive impedance (X_L), the overall circuit exhibits capacitive characteristics, causing the voltage to lag behind the current. Conversely, when X_L exceeds X_C, the circuit becomes inductive, resulting in the voltage leading the current. At resonance, where X_L equals X_C, the voltage and current are in phase, and the circuit's impedance reaches its minimum. Both X_L and X_C are dependent on the frequency of the source.

However, in the absence of an external source, the system oscillates at its natural frequency $\omega_0 = \frac{1}{\sqrt{LC}}$. This indicates that the time required for the capacitor to discharge is the same as the time needed for the inductor to allow the current to reach its maximum value.

In the context of buildings, the voltage source is represented by the difference between indoor and outdoor temperatures. Since temperature changes occur gradually, it can be assumed that the walls transition from one steady state to another, with the external temperature changes occurring at a frequency close to zero.

The thermal analogy indicates that heat storage and heat flow must exhibit the same time delay. In the heat velocity formula $c = \sqrt{\frac{k_\sigma}{\rho c_{sp} \tau_o}}$ the characteristic time τ_o governs these two phenomena to ensure they work together, enabling heat to flow in the shortest possible time.

The characteristic time for a common wall with two brick layers, plaster and a layer of extruded polystyrene isolation is about 2.5h and the whole time needed for the one side to “feel” a thermal pulse on the other side and equilibrate is more than a day.

5.2. Internal surfaces of symmetry

It is worthwhile to examine the internal symmetry of temperatures at various points within the solid. The temperature function $f(x, y, z)$ $(\text{when } t \to \infty)$ exhibits symmetrical values relative to a specific surface, known as surface symmetry, located in the interior of the solid. This surface represents the geometric locus of points with an average temperature and is planar when two opposing sides of the body are in a steady state (see Figure 13(a)). When more sides are in a steady state, the function values reveal symmetry about an axis (axis symmetry). In cases with more fixed sides, the temperature values also demonstrate axis symmetry, showing a distribution around a non-planar surface (see Figure 13(b)).

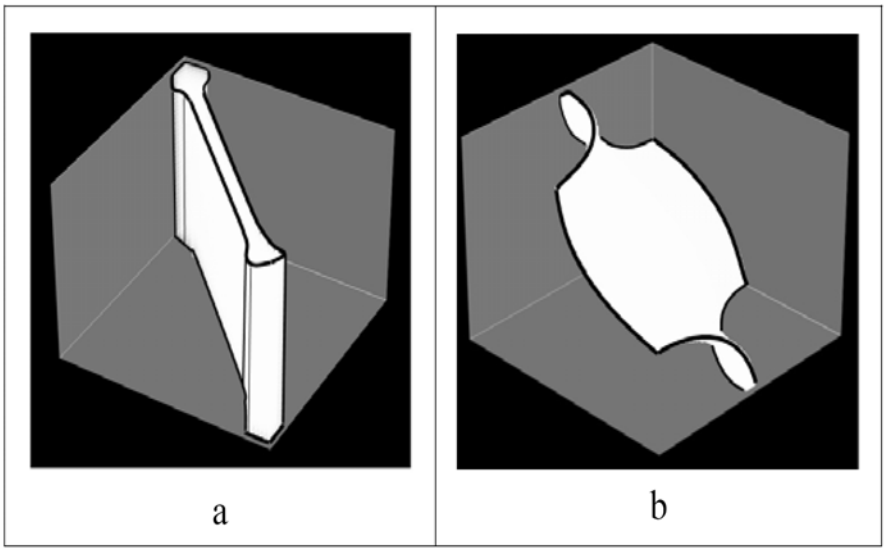

Figure 13. Plane (a) and curved (b) internal surface with average temperature.

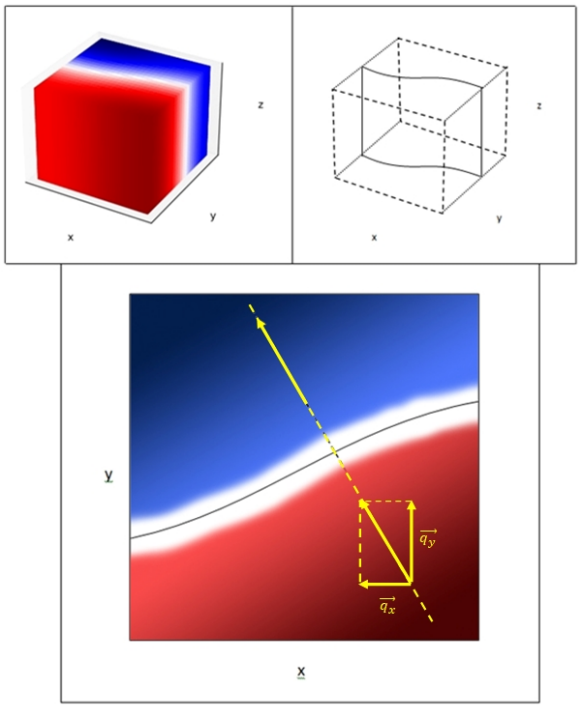

Figure 14. Components of heat flux (*x*-*y* axes).

When a "white surface" exhibits a small radius of curvature, there is an increased temperature gradient on its concave side (the inner surface). The center of curvature of this surface indicates the direction of significant heat flow (see Figure 14).

It is important to note that the assumed heat "point-source" may not be singular and could potentially reside outside the solid. When the thermal field is homogeneous, the radius of curvature becomes infinite. As the solid approaches its final state, these temperature regions either expand throughout the body or shift and diminish, ultimately leading to a thermal equilibrium at a temperature that is either higher or lower than the average.

5.3. The building shell

The same principles apply within a building's envelope. Generally, the temperature across the entire external surface of each wall tends to be

uniform, creating a homogeneous field of external temperatures. There are no significant point sources of heat outside the building. As a result, almost vertical isothermal surfaces develop on the side walls. This phenomenon is similarly observed at the base of the building, where the ground maintains a consistent temperature throughout its area.

In practical scenarios, shading emerges as a crucial factor that can significantly influence a building's energy efficiency. By optimizing orientation and shading, the energy required for both heating and cooling can be effectively controlled and managed.

Doubling the thickness of a wall-without altering its construction material-would result in a quadrupling of the time needed for its temperature to change. The duration of heat transfer from one side to the other is determined solely by the length of that particular side, independent of the lengths of the other sides. Therefore, it is possible to analyze the time on each axis individually. The presence of large dimensions on the other axes influences their own respective times, thereby affecting the overall maximum time required to achieve a stable final temperature, expressed as $t_{xyz} = \max(t_x, t_y, t_z)$.

A shell is defined as a closed surface that encapsulates a volume. In the context of the SoTV application, the shell under consideration is a parallelepiped that is completely sealed without any openings.

Then, input dimensions akin to those of a building, treating the shell as a structure. For each face of the shell a U_{VALUE} must be specified, the thickness of the shell, and the overall dimensions of the parallelepiped. Additionally, there is the option to incorporate thermal transition resistances for each face into the application's calculations.

For the sake of illustration, let us assume an empty parallelepiped with dimensions of $1 \times 1 \times 1\,\mathrm{m}$ and a thickness of 0.1 m for each face. It is also assumed a $U_{VALUE} = 1$ for all surfaces.

Initially, it will be determined the power required to maintain an internal temperature of $u_{in} = 1^{\circ}\mathrm{C}$ while the external temperature is $u_{out} = 0^{\circ}\mathrm{C}$ across all faces. The power needed to maintain this temperature difference $(\Delta u = 1^{\circ}\mathrm{C})$ is calculated to be $P = 0.002\,\mathrm{kW}$.

By varying these parameters, the following results were observed: The power required is directly proportional to the temperature difference $|\Delta u|$. As the difference between the internal and external temperatures increases, so does the power needed for heating or cooling the interior space. Thus, the power expenditure is directly related to this temperature disparity.

The thickness of each face is significant only insofar as it influences the calculation of the material's thermal resistance. This implies that if it is assigned different thicknesses to the various sides of the parallelepiped while keeping the U_{VALUE} coefficients constant, the energy required for heating or cooling each face will remain unchanged. Even though the thickness of the shell has been altered, it has been defined its thermal resistance to be equivalent.

The dimensions of the faces play a crucial role as they determine the cross-sections through which energy can flow. An increase in each dimension of the solid by a factor of ten escalates the volume by $10^3 = 1000$ times; however, it only increases the required power by $10^2 = 100$ times, since power relates to area, not volume.

Doubling the U_{VALUE} effectively doubles the necessary power.

For instance, consider a building with three floors measuring $10 \times 10 \times 10$ meters. With an older masonry construction comprising plaster, two rows of bricks, and extruded polystyrene, the thermal transmittance coefficient (U_{VALUE}) would be 0.88 (with a total thickness of 0.25 m). In contrast, a new masonry version that includes the same materials plus an air layer results in a U_{VALUE} of 0.44. This reduction in thermal transmittance alters the total required power (for a temperature differential of 1°C),

changing it from $P = 0.176\,\text{kW}$ to $P = 0.088\,\text{kW}$. On an average winter day, with an ambient temperature of 8°C and a thermostat setting of 22°C, the difference in required power reaches 1.23 kW. Over the course of a month, this variation can accumulate to hundreds of kWh for a bigger building.

If moisture is present in air-exposed areas of even modern masonry, then a mere 1 mm thickness of moisture can lead to an increased energy requirement of 0.048 kWh per day for a temperature differential of just $\Delta u = 1^{\circ}\text{C}$. For instance, on a typical winter day with an outdoor temperature of 8°C and an indoor thermostat setting of 22°C, this results in an approximate energy increase of 0.7 kWh. The impact is even more significant in older buildings.

It is clear that the choice of insulating materials can significantly influence the energy efficiency of a building, even with minimal thickness. When 5% of a wall's total thickness consists of insulating material, the energy needed for cooling or heating the building can be halved.

Air serves as a highly effective insulator, being 30 times more proficient in insulation than brick. However, the presence of moisture within the wall can alter this scenario. Moisture can accumulate at the junctions of different materials, not just on the exterior of the masonry. During winter, when the outside temperature is 8°C and the inside temperature rises to 22°C, a significant amount of moisture - exceeding 60% - can lead to condensation within the masonry. When air becomes moist, our heating energy requirements increase substantially. For instance, a 10% rise in humidity within the masonry results in a 6.5% increase in energy consumption for heating.

6. Conclusions

The thermal strings model forecasts the relaxation time required for a solid body to achieve equilibrium and the power necessary to maintain it in a non-equilibrium state. Notably, these predictions align with those from the

diffusion model. The thermal strings model provides a mathematical framework that facilitates rapid calculations in three dimensions.

In practical applications of SoTV, nearly all predictions have been confirmed. Time measurements are precise, and the outcomes correspond not only to thermal strings theory in 3D but also to the classical diffusion theory.

Key findings indicate that the thickness of the solid significantly influences heat transfer time. Moreover, the interplay of density, specific heat capacity, and thermal conductivity is crucial for the temporal variations in temperature. It is important to note that thermal conductivity acts competitively against the thermal inertia of the solid [19-21].

The time required for heat transfer can be modified with appropriate materials, and it can be significantly extended if it is aimed to ensure that the interior of a building remains unaffected by fluctuations in outside temperatures [22].

The energy transferred through a solid substance is influenced by the boundary conditions, particularly when certain sides are maintained at a constant temperature. In such instances, it takes four times longer for energy to be transferred, allowing the body to reach its final thermal state.

A solid body achieves thermal equilibrium when all its parts attain the same temperature, which may or may not coincide with the average temperature of its boundaries and once equilibrium is reached, heat conduction ceases.

However, if two opposite sides of the body are maintained at constant but unequal temperatures, then equilibrium cannot be achieved, leading to a situation where the temperature differs across various points within the body. Consequently, there will be continuous heat transfer from the hotter regions to the colder ones, necessitating that we provide ongoing energy through some external mechanism.

Moreover, discrepancies may arise between the theoretical predictions and the actual results depending on the initial temperatures of the boundaries. When these temperatures are very close to the final temperature, the

relaxation time is typically shorter than anticipated, while a greater disparity results in a longer relaxation time.

References

[1] Liqiu Wang, Xuesheng Zhou and Xiaohao Wei, Heat Conduction - Mathematical Models and Analytical Solutions, Berlin Heidelberg: Springer-Verlag, 2008. DOI: https://doi.org/10.1007/978-3-540-74303-3.

[2] N. Yu, S. Imatani and T. Inoue, Characteristics of temperature field due to pulsed heat input calculated by non-Fourier heat conduction hypothesis, JSME International Journal Series A-Solid Mechanics and Material Engineering 47(4) (2004), 574-580. DOI: https://doi.org/10.1299/jsmea.47.574.

[3] E. Marín, Basic Principles of Thermal Wave Physics and Related Techniques, Chapter I in Thermal Wave Physics and Related Photothermal Techniques: Basic Principles and Recent Developments, Ernesto Marín Moares, editor, (Transworld Research, Kerala, India) 2009, pp. 1-28.

[4] D. Y. Tzou, Damping and resonance phenomena of thermal waves, ASME Journal of Applied Mechanics 59 (1992c), 862-867. DOI: https://doi.org/10.1115/1.2894054.

[5] D. Y. Tzou, Macro-to Microscale Heat Transfer: The Lagging Behavior, Second Edition, John Wiley & Sons, 2015, pp. 62-116. DOI: https://doi.org/10.1002/9781118818275.

[6] S. Rouchier, Solving inverse problems in building physics: an overview of guidelines for a careful and optimal use of data, Energy and Buildings 166 (2018), 178-195. DOI: https://doi.org/10.1016/j.enbuild.2018.02.009.

[7] Hossein Askarizadeh, Ehsan Baniasadi and Hossein Ahmadikia, Equilibrium and non-equilibrium thermodynamic analysis of high-order dual-phase-lag heat conduction, International Journal of Heat and Mass Transfer 104 (2017), 301-309. DOI: http://dx.doi.org/10.1016/j.ijheatmasstransfer.2016.08.060.

[8] J. Crank and P. Nicolson, A Practical Method for Numerical Evaluation of Solutions of Partial Differential Equations of the Heat-conduction Type, Cambridge University Press, 2008. DOI: https://doi.org/10.1007/BF02127704.

[9] Da Yu Tzou, The generalized lagging response in small-scale and high-rate heating, International Journal of Heat and Mass Transfer 38(17) (1995), 3231-3240. DOI: https://doi.org/10.1016/0017-9310(95)00052-B.

[10] Franca Franchi, Angelo Morro-global existence and asymptotic stability in nonlinear heat conduction, Journal of Mathematical Analysis and Application (1994), 594-601. DOI: https://doi.org/10.1006/jmaa.1994.1447.

[11] M. N. Ozisik and D. Y. Tzou, On the wave theory in heat conduction, Journal of Heat Transfer 116/527 (1994), 529-532. DOI: https://doi.org/10.1115/1.2910903.

[12] J. Ordóñez-Miranda and J. J. Alvarado-Gil, Thermal wave oscillations and thermal relaxation time determination in a hyperbolic heat transport model, International Journal of Thermal Sciences 48(11) (2009), 2053-2062. DOI: https://doi.org/10.1016/j.ijthermalsci.2009.03.008.

[13] Rainer Krankenhagen, Florian Jonietz and Stefan Zirker, Determination of thermal parameters of concrete by active thermographic measurements, J. Nondestruct. Eval. 41(25) (2022), 1-13. DOI: https://doi.org/10.1007/s10921-022-00861-6.

[14] M. Giglio and A. Vendramini, Thermal-diffusion Measurements near a Consolute Critical Point, 1975. DOI: https://doi.org/10.1103/PhysRevLett.34.561.

[15] H. S. Carslaw and J. C. Jaeger, Conduction of Heat in Solids, Oxford University Press, U. S. A., 1959.

[16] T. O. T. E. E. 20701-2/2010: Thermophysical properties of building materials and control of the thermal insulation adequacy of buildings (TEE 2010)-Greece.

[17] T. O. T. E. E. 20701-1/2010: Detailed national specifications of parameters for calculating the energy efficiency of buildings and issuing an energy efficiency certificate (TEE 2012 - 2nd edition), Greece.

[18] ASHRAE-Physical Properties of Materials- https://www.ashrae.org/.

[19] Lahcene Bellahcene, Ali Cheknane, S. M. A. Bekkouche and Djemal Sahel, The effect of the thermal inertia on the thermal transfer in building wall, International Conference on Advances in Energy Systems and Environmental Engineering (ASEE17), 2017. DOI: 10.1051/e3sconf/20172200013.

[20] Jaroslav Šesták, Dynamic character of thermal analysis where thermal inertia is a real and not negligible effect influencing the evaluation of non-isothermal kinetics: A Review, 2021. DOI: https://doi.org/10.3390/thermo1020015.

[21] M. S. Veto and P. R. Christensen, Mathematical Theory of Thermal Inertia Revisited 1: Improving Our Understanding of Martian Thermophysical Properties Through Analogous Examples of Periodic Diffusive Inertias, Arizona State University, 2015.

[22] Dongliang Zhao, Xin Qian, Xiaokun Gu, Saad Ayub Jajja and Ronggui Yang, Measurement Techniques for Thermal Conductivity and Interfacial Thermal Conductance of Bulk and Thin Film Materials, 2016. DOI: http://dx.doi.org/10.1115/1.4034605.